Uniformly spaced λ/4-shifted Bragg grating array with wafer-scale CMOS-compatible process

8 authors, including:

Jie Sun
Massachusetts Institute of Technology
54 PUBLICATIONS **661** CITATIONS

SEE PROFILE

Purnawirman Purnawirman
Massachusetts Institute of Technology
18 PUBLICATIONS **65** CITATIONS

SEE PROFILE

Ehsan shah hosseini
Massachusetts Institute of Technology
75 PUBLICATIONS **552** CITATIONS

SEE PROFILE

Douglas D. Coolbaugh
University at Albany, The State University o…
79 PUBLICATIONS **824** CITATIONS

SEE PROFILE

Uniformly spaced λ/4-shifted Bragg grating array with wafer-scale CMOS-compatible process

Jie Sun,[1,*] Purnawirman,[1] Ehsan Shah Hosseini,[1] Jonathan D. B. Bradley,[1] Thomas N. Adam,[2]
Gerald Leake,[2] Douglas Coolbaugh,[2] and Michael R. Watts[1]

[1]*Research Laboratory of Electronics, Massachusetts Institute of Technology, Cambridge, Massachusetts 02139, USA*

[2]*College of Nanoscale Science and Engineering, University at Albany, Albany, New York 12203, USA*

Corresponding author: sunjie@mit.edu

We report on an integrated λ/4-shifted Bragg grating array using a wafer-scale complementary metal-oxide semi-conductor (CMOS) compatible process with silicon–nitride waveguides. A sidewall grating was used to simplify the fabrication process, and a sampled Bragg grating with equivalent phase-shift structure was employed to achieve an accurate λ/4 phase shift. A four-channel λ/4-shifted Bragg grating array with highly uniform channel spacing was demonstrated with a measured channel spacing variation below 10 pm (1.25 GHz). The high channel-spacing uniformity and the CMOS-compatibility of the demonstrated device hold promise for integrated distributed feedback laser arrays for various silicon photonic applications.   © 2013 Optical Society of America

OCIS codes: (130.3120) Integrated optics devices; (050.5080) Phase shift; (050.2770) Gratings.

http://dx.doi.org/10.1364/OL.38.004002

Taking advantage of well-established wafer-scale complementary metal-oxide semiconductor (CMOS) fabrication techniques, silicon photonics have shown remarkable large-scale integration capabilities [1] with applications ranging from long-haul telecommunications to short-reach data communications. To further integrate light sources onto the silicon photonic chip, erbium-doped waveguide lasers have been demonstrated [2] as a potential integration scheme, among other approaches such as hybrid silicon III–V integration [3]. As a step further toward the large-scale-integrated silicon photonic light sources, we recently demonstrated the erbium-doped waveguide lasers in a 300 mm wafer-scale CMOS-compatible process [4]. To ensure single-frequency, narrow linewidth operation, quarter-wave (λ/4) shifted Bragg gratings are seen as a key component of future directly integrated, single-wavelength lasers [2,5,6]. Furthermore, in wavelength division multiplexed (WDM) communications, an array of λ/4-shifted Bragg gratings enables multiple channels with uniformly spaced wavelengths aligned with the WDM grid, which is indispensible for high-capacity optical communications. Traditionally, the λ/4-shifted grating is made by phase-shifting the grating by a quarter of the resonant wavelength λ [5], which, although widely used in manufacturing semiconductor distributed feedback (DFB) laser diodes, exhibits poor tolerances due to the stringent fabrication accuracy required to make such phase-shift structures. As a result, it is extremely challenging to make quarter-wave-shifted Bragg grating arrays with uniform wavelength spacings. To overcome this challenge, sampled Bragg gratings with an equivalent quarter-wave phase shift in the sampling function have been proposed to more accurately control the phase-shift, a technique demonstrated in fiber Bragg gratings [7,8], III–V laser diodes [9], and recently in silicon waveguide [10]. However, in all of these equivalent phase-shift demonstrations, interference lithography was required to pattern the gratings because of the excellent grating coherence it offers; however, interference lithography is not used

within CMOS processes where optical projection lithography reigns exclusively for wafer-scale processing.

In this Letter, we demonstrate a four-channel λ/4-shifted Bragg grating array with highly uniform channel spacing, using the equivalent phase-shift method and state-of-the-art 300 mm CMOS fabrication processes. A uniformly spaced quarter-wave-shifted Bragg grating array is obtained where the measured channel-spacing difference is below 10 pm (1.25 GHz), which is promising for the future large-scale integration of multiwavelength laser arrays for silicon photonic applications.

Figure 1(a) shows the schematic of the four-channel quarter-wave-shifted Bragg grating array composed of
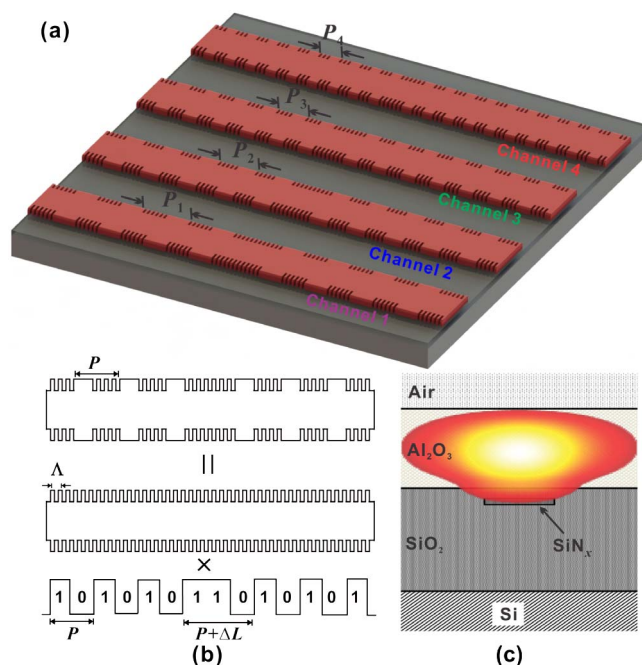
Fig. 1.   (a) Schematic of the four-channel λ/4-shifted Bragg grating array with equivalent phase shift. (b) An illustration of the equivalent phase-shift method. (c) The cross section and the simulated mode profile of the waveguide structure.

four sampled Bragg gratings with equivalent phase-shift structure. Figure 1(b) illustrates the equivalent phase-shift method, which can be seen as a uniform grating (grating pitch Λ) sampled or on–off modulated by a quasi-periodic sampling function with sampling period P ($P \gg \Lambda$). Figure 2 simulates the typical grating transmission spectrum of the sampled Bragg grating structure shown in Fig. 1(b). Similar to the sampled fiber Bragg gratings [7,8], the sampling on a uniform grating created multiple resonant orders in the resulting grating spectrum. The wavelength spacing $\Delta\lambda$ between the resonant orders is given by [11]

$$\Delta\lambda = \frac{\lambda_0^2}{2n_g P}, \tag{1}$$

where λ_0, the wavelength of the 0th resonant order, is set by the Bragg condition $\lambda_0 = 2n_{\text{eff}}\Lambda$ and n_{eff} is the effective refractive index of the waveguide. n_g is the group index of the waveguide. It is noted in Fig. 1(b) that the sampling function is phase-shifted in the center by a distance ΔL, which creates an equivalent phase-shift $\Delta\phi$ in the −1st resonant order. $\Delta\phi$ is given by [7]

$$\Delta\phi = \frac{2\pi\Delta L}{P}. \tag{2}$$

Accordingly, a quarter-wave phase shift is generated when $\Delta L = P/2(\Delta\phi = \pi)$, as shown in the inset of Fig. 2(a).
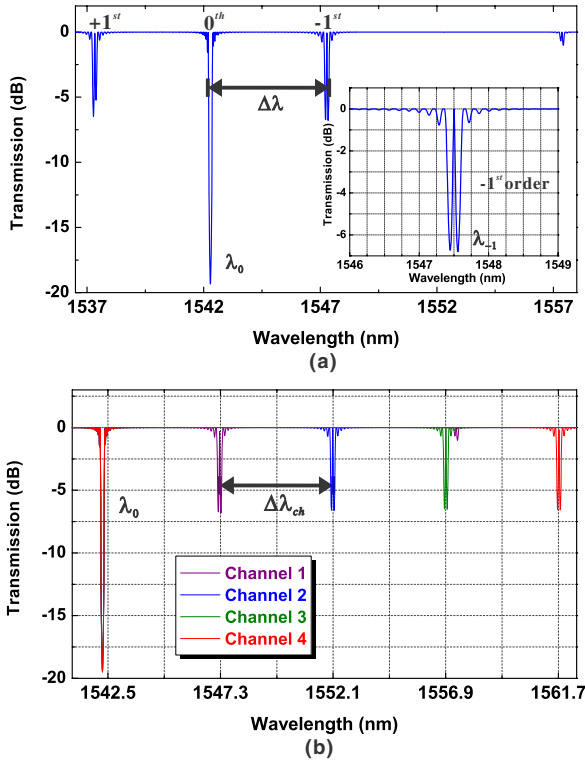
The advantage of using the equivalent phase-shift structure over the conventional phase shift is twofold. First, as indicated by Eq. (2), in the equivalent phase-shift structure, the phase shift is introduced by phase shifting a sampling function with a much larger period (P) than the grating period itself (Λ), and the phase shift is therefore easier to be precisely controlled. Second, as given by Eq. (1), the wavelength spacing $\Delta\lambda$ between the phase-shift resonance in the −1st-order (λ_{-1}) and the Bragg wavelength (λ_0) is related to the sampling period P; therefore an array of quarter-wave-shifted Bragg gratings can be formed by stepping the relatively large sampling period P. When an array of such waveguides with the same uniform gratings are placed close to each other, so that Λ and n_{eff} can be considered the same after fabrication, as shown schematically in Fig. 1(a), the wavelength spacing of resonances of adjacent sampled Bragg gratings in the array, or the channel spacing $\Delta\lambda_{\text{ch}}$ of the array, is given by

$$\Delta\lambda_{\text{ch}} = \frac{\lambda_0^2}{2n_g}\left(\frac{1}{P_i} - \frac{1}{P_{i+1}}\right), \tag{3}$$

where P_i is the sampling period of the ith channel. Since Λ and n_{eff} can be considered the same within the array, highly uniform channel spacing can be achieved because the sensitivity to the fabrication variations has been reduced by a factor of about $(P/\Lambda)^2$ ($P \gg \Lambda$), and the relatively large sampling period P can be accurately controlled in fabrication. Figure 2(b) simulated a four-channel $\lambda/4$-shifted Bragg grating array by stepping the sampling period P.

The proposed $\lambda/4$-shifted Bragg grating array was fabricated in a 300-mm CMOS foundry at 65-nm technology node using 193-nm optical immersion lithography. The cross section of the waveguide is illustrated in Fig. 1(c), where SiN_x made from the plasma-enhanced chemical vapor deposition serves as the waveguide core with 4 μm width and 100 nm thickness. Sidewall gratings with a width of 0.5 μm on both edges are used here, so that the waveguide and the gratings can be patterned within a single lithography step [12]. The grating has a pitch $\Lambda = 482$ nm and a 0.5 duty cycle. Figure 3 shows the scanning-electron micrographs of the fabricated sampled Bragg grating. A layer of 180 nm SiO_2 was then deposited on top of the SiN_x waveguide, followed by another deposition of 1.3 μm Al_2O_3. Using a finite difference mode solver, the calculated effective index of the waveguide is $n_{\text{eff}} = 1.60$, corresponding to the Bragg

Fig. 2. (a) Simulated transmission spectrum of a typical sampled Bragg grating with a phase shift in the sampling function. Inset: a close-up view of the −1st resonant order showing a quarter-wave phase-shift resonance in the center. (b) An example of a four-channel $\lambda/4$-shifted Bragg grating array with uniform channel spacing $\Delta\lambda_{\text{ch}}$.
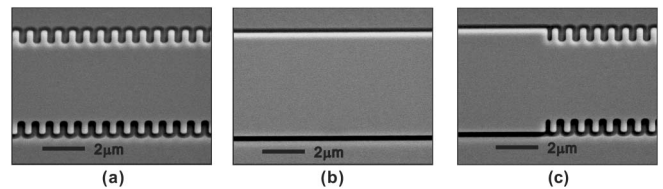
Fig. 3. Scanning-electron micrographs of the fabricated sampled Bragg grating in a standard CMOS foundry using optical lithography. (a) The section with sidewall Bragg gratings when the sampling is on. (b) The section with pure waveguide when the sampling is off. (c) The transition section mixed with waveguide and Bragg gratings.
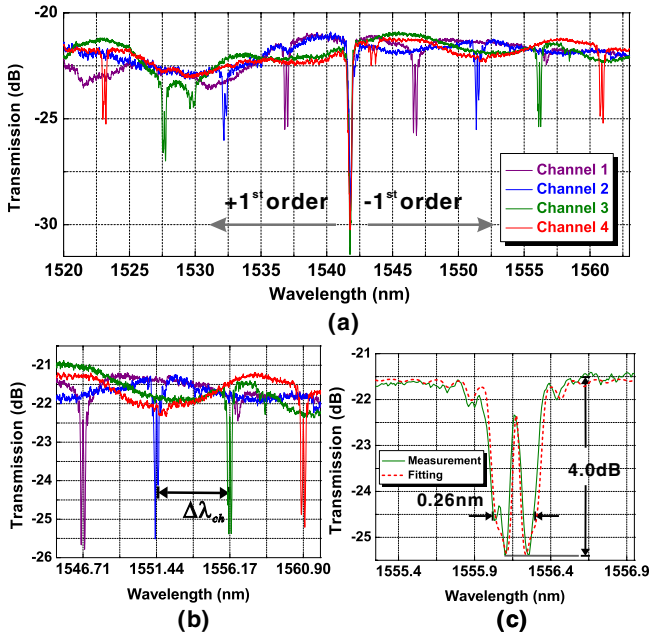
Fig. 4. (a) Measured transmission spectra of the fabricated four-channel $\lambda/4$-shifted Bragg grating array. (b) The −1st resonant order of the transmission spectra. (c) A close-up view of the phase-shift resonance of channel 3. Dotted line: the fitted curve.

wavelength $\lambda_0 = 1542.4$ nm in the 0th-order, and the group index is $n_g = 1.67$. The sampling period P_i is 142.8, 72.94, 49.0, and 36.9 μm to form a uniformly spaced four-channel array of $\lambda/4$-shifted Bragg grating with 4.77 nm channel spacing according to Eq. (3). It is seen the sampling period is much larger than the grating period ($P/\Lambda \sim 100$), offering accurate control over the phase shift and channel spacing uniformity. The total length of the fabricated gratings is around 10 mm for all of the four channels.

The fabricated $\lambda/4$-shifted Bragg grating array was measured with a tunable laser with 10 pm wavelength resolution and ± 3.6 pm accuracy, using cleaved fiber to couple light into and out of the photonic chip at transverse-electric polarization. Figure 4 shows the measured transmission spectra of all of the four channels. As seen in Fig. 4(a), several resonant orders appear in the transmission spectrum, similar to the simulation in Fig. 2(a). Figure 4(b) shows the measured transmission spectra of −1st resonant order. The quarter-wave-shifted resonance occurs at 1546.71, 1551.44, 1556.17, and 1560.90 nm, corresponding to an averaged channel spacing 4.73 nm with channel-spacing variation less than 10 pm (1.25 GHz), which is below the resolution of the tunable laser. It is also noted that the Bragg wavelengths (the center wavelength of the 0th resonant order) of all four channels are aligned at $\lambda_0 = 1541.8$ nm, meaning the grating pitch Λ and n_{eff} are statistically the same for all four channels because of their spatial proximity on the chip. Moreover, the channel spacing is highly uniform, highlighting the advantage of the equivalent phase-shift method with the aide of 193 nm immersion lithography and 300 mm CMOS processing techniques. Figure 4(c) shows a close-up view of channel 3 where a resonance caused

by an accurate quarter-wave phase shift is observed in the −1st resonant order. The extinction of the resonance is 4.0 dB, and the bandwidth is 0.26 pm (32.5 GHz). By fitting to the measured grating spectrum, the calculated coupling coefficient of the grating is 5.6 cm^{-1}. A stronger grating and hence a larger extinction can be achieved by increasing the width of the grating. The estimated propagation loss is 2.4 dB/cm, mainly due to the material loss in the Al_2O_3 cladding. The scattering loss from the grating should be minimal in such a Bragg grating with weak perturbation. An on-chip DFB laser array with uniform wavelength spacing can be expected based on the demonstrated quarter-wave-shifted Bragg grating array, combined with our wafer-scale CMOS-compatible integrated erbium-doped laser platform [4].

In this Letter, we demonstrated a four-channel $\lambda/4$-shifted Bragg grating array fabricated in a CMOS-compatible SiN_x process using 193-nm immersion lithography. Sidewall gratings were employed to simplify the grating fabrication, and the equivalent phase-shift method was utilized to better control the uniformity of the channel spacing. Highly uniform channel spacing was achieved with variations below 10 pm. The CMOS-compatibility of the process, and the high uniformity of the channel spacing of the demonstrated $\lambda/4$-shifted array, is promising for the future development of multiwavelength-integrated DFB laser arrays enabling high-quality WDM light sources for silicon photonic applications as well as other integrated resonant devices such as Bragg-grating-based electro-optic resonant modulator arrays.

References
1. J. Sun, E. Timurdogan, A. Yaacobi, E. S. Hosseini, and M. R. Watts, Nature **493**, 195 (2013).
2. E. H. Bernhardi, H. A. G. M. van Wolferen, L. Agazzi, M. R. H. Khan, C. G. H. Roeloffzen, K. Wörhoff, M. Pollnau, and R. M. de Ridder, Opt. Lett. **35**, 2394 (2010).
3. A. W. Fang, H. Park, O. Cohen, R. Jones, M. J. Paniccia, and J. E. Bowers, Opt. Express **14**, 9203 (2006).
4. Purnawirman, J. Sun, T. N. Adam, G. Leake, D. Coolbaugh, J. D. B. Bradley, E. Hosseini, and M. R. Watts, Opt. Lett. **38**, 1760 (2013).
5. K. Utaka, S. Akiba, K. Sakai, and Y. Matsushima, IEEE J. Quantum Electron. **22**, 1042 (1986).
6. A. W. Fang, E. Lively, Y. H. Kuo, D. Liang, and J. E. Bowers, Opt. Express **16**, 4413 (2008).
7. Y. Dai, X. Chen, D. Jiang, S. Xie, and C. Fan, IEEE Photon. Technol. Lett. **16**, 2284 (2004).
8. J. Sun, Y. Dai, X. Chen, Y. Zhang, and S. Xie, IEEE Photon. Technol. Lett. **18**, 2493 (2006).
9. Y. Shi, X. Chen, Y. Zhou, S. Li, L. Lu, R. Liu, and Y. Feng, Opt. Lett. **37**, 3315 (2012).
10. J. Sun, C. W. Holzwarth, and H. I. Smith, IEEE Photon. Technol. Lett. **24**, 25 (2012).
11. V. Jayaraman, Z.-M. Chuang, and L. A. Coldren, IEEE J. Quantum Electron. **29**, 1824 (1993).
12. M. Belt, J. Bovington, R. Moreira, J. F. Bauters, M. J. R. Heck, J. S. Barton, J. E. Bowers, and D. J. Blumenthal, Opt. Express **21**, 1181 (2013).